

# Digital Nonlinearity Compensation Techniques for Unrepeated Optical Systems

José Hélio da Cruz Júnior, Tiago Sutili, Lucas Silva Schanner,  
Sandro Marcelo Rossi, and Rafael Carvalho Figueiredo

**Abstract**—In this paper, we experimentally investigate the performance of unrepeated optical transmission comparing different nonlinear compensation (NLC) implementations. Specifically, digital back-propagation (DBP) algorithm and maximum likelihood sequence estimation (MLSE) are applied for intra-channel NLC with and without  $4 \times 4$  multiple-input multiple-output (MIMO) equalization. Both NLC algorithms are evaluated in an unrepeated WDM transmission of  $17 \times 200$ -Gb/s channels (32 GBd DP-16QAM) over 350 km of large effective area and low loss single-mode fibers. The results indicate a  $Q^2$  factor and optimum launch power improvements of up to 0.4 dB and 2 dB, respectively, compared to the linear compensation (LC), combining MLSE and DBP with MIMO equalization.

**Keywords**—Digital back-propagation, maximum likelihood sequence estimation, nonlinear compensation, unrepeated systems.

## I. INTRODUCTION

Unrepeated optical systems [1] allows high-capacity transmission (up to dozens of terabits per second) through long-reach links (up to hundreds of kilometers) employing advanced amplification techniques to avoid the need of electrical feeding along the link. Usually, this is accomplished with amplification schemes based on remote optically pumped amplifiers (ROPAs) and/or distributed Raman amplifiers (DRAs). ROPAs employ a few meters of Erbium-doped fibers (EDFs) with a gain mechanism similar to the one that occurs on conventional Erbium-doped fiber amplifiers (EDFAs). DRAs allow energy to be transferred to the propagating channels through nonlinear interactions based on the Raman scattering phenomena. In both cases, pumping units are positioned close to the transmitter and/or receiver terminals, with the pumping power being propagated through the same fiber than the propagating channels or through a dedicated link. However, due to the complex amplification scheme, the link design is an intricate process [2], demanding complex optimization algorithms [3] or, even, approaches based on artificial intelligence [4].

To fully optimize an unrepeated optical link, besides the maximization of the received optical signal-to-noise ratio (OSNR), one must avoid nonlinear degradation by limiting the maximum propagation power of each channel to values

below the fiber nonlinear threshold along the link. Power values above this limit will induce Kerr related effects, which, on a practical wavelength-multiplexed system, will degrade the propagating channels through both self-phase modulation (SPM) and cross-phase modulation (XPM). However, since the power profile of each channel depends on a series of systemic characteristics, it is hard to ensure that the system will always operate with all channels within the maximum propagation power limit. Furthermore, if a higher maximum propagation power is allowed, the reach and/or capacity of the link can be significantly improved. Thus, it may be advantageous to implement some kind of nonlinear compensation (NLC) in the digital signal processing (DSP) domain, even considering the high complexity of this kind of algorithm [5].

Among the nonlinear equalization algorithms proposed in the literature, the digital back-propagation (DBP) [6] allows one to evaluate the degradation suffered by each channel by modeling its propagation power profile from the receiver to the transmitter in steps of a few kilometers. Alternatively, another technique to compensate nonlinear effects is the maximum likelihood sequence estimation (MLSE) [7], on which conditional probability density functions (PDF) are employed to describe the signal as a conditional sequence, rather than as individual symbols. However, a training process is required to define the channel statistics and to estimate its conditional PDFs. After the training step, the maximum likelihood criterion can be applied to estimate the sequence of received symbols. In this context, previous works have investigated different NLC techniques. On one hand, the benefits of DBP, symbol-rate optimization (SRO), and probabilistic shaping (PS) are experimentally evaluated for ultra-long-haul optical transmission [8]. On the other hand, the MLSE performance is numerically investigated for intra-channel NLC [7] and the performance of MLSE and DBP are numerically analyzed for superchannel transmission [9] with different modulation formats and spectral shaping. However, whereas an unrepeated system was employed in this work, all the previous ones considered repeated optical transmission scenarios.

In this work, we experimentally investigate an unrepeated optical transmission comparing the NLC performance for several implementations that combine DBP and MLSE with and without a  $4 \times 4$  multiple-input multiple-output (MIMO) equalizer. The analysis, as described in Section II, is based on the unrepeated wavelength-division multiplexed (WDM) transmission of  $17 \times 200$ -Gb/s channels over 350 km of large-effective area and low-loss single-mode

J. H. Cruz Júnior, T. Sutili, L. S. Schanner, S. M. Rossi, and R. C. Figueiredo are with the Optical Communication Solutions, CPQD, Campinas-SP, e-mail: hcruz@cpqd.com.br; tsutili@cpqd.com.br; schanner@cpqd.com.br; sandro@cpqd.com.br; and, rafaelcf@cpqd.com.br.

This work was partially supported by the Brazilian MCTIC and FUNTTEL-Finep.

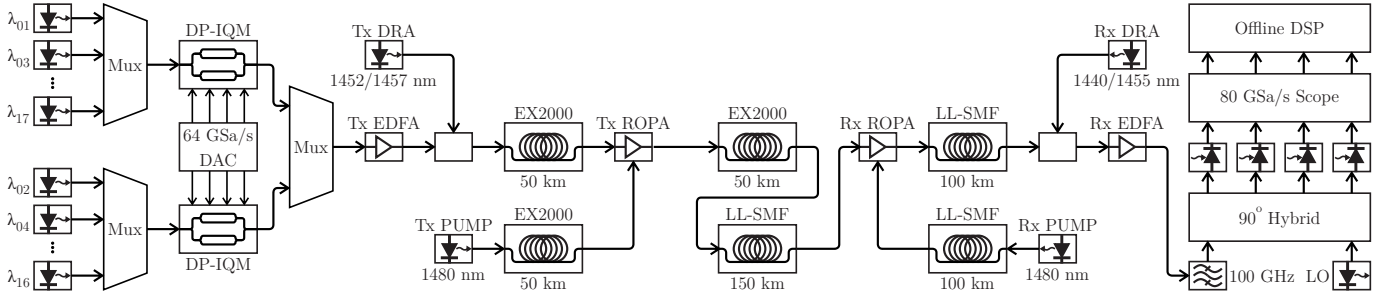


Fig. 1. Experimental unrepeated setup encompassing the transmission of  $17 \times 200$ -Gb/s channels over a 350-km heterogeneous link employing hybrid (DRAs combined with EDFAs) and remote (ROPAs) amplification.

fibers (LL-SMF). The experimental results, as discussed in Section III, indicate a  $Q^2$  factor and optimum launch power improvements of up to 0.4 dB and 2 dB, respectively, compared to the linear compensation (LC), through the combination of both MLSE and DBP with MIMO equalization. Finally, Section IV presents the conclusions of the work.

## II. EXPERIMENTAL SETUP

The experimental data, used in the NLC analysis, were acquired employing the setup presented in Fig. 1 [5], encompassing the transmission of 17 wavelength-multiplexed channels divided into two interleaved sets. The outputs of a digital-to-analog converter (DAC) are employed to independently modulate each interleaved set through dual-polarization in-phase and quadrature modulators (DP-IQM), resulting in 200-Gb/s (32 GBd) dual-polarization (DP) quadrature amplitude modulated (QAM) channels with constellations composed of 16 symbols (DP-16QAM). Following, both sets are combined by a multiplexer and amplified in the transmitter hybrid amplification stage, which is composed by a conventional EDFA booster (Tx EDFA) and a transmitter distributed Raman amplifier (Tx DRA). The transmitter distributed Raman amplification takes place on the first 50-km of large-effective area low-loss fiber (EX2000), which allows higher propagation powers without inducing nonlinear phenomena related to the Kerr effect. The transmitter amplification scheme is completed by a forward-pumped remote optically pumped amplifier (Tx ROPA), whose pumping optical power is delivered by a dedicated 50-km EX2000 span. Next, the signal is propagated

over a 200-km intermediate span, encompassing a 50-km EX2000 span after the transmitter-side ROPA (since the high signal power in this region could also induce nonlinear degradation), followed by 150-km of low-loss single-mode fiber (LL-SMF). On the receiver side, first the channel set is amplified by a backward-pumped ROPA (Rx ROPA), again employing a dedicated span to deliver pumping optical power, and by a second stage of distributed Raman amplification (Rx DRA). The backward propagating Raman pumping unit is located close to the receiver terminal, jointly with a conventional EDFA pre-amplifier (Rx EDFA). Finally, the central channel under test is selected and coherently received through its mixing with a local oscillator in the  $90^\circ$  optical hybrid and the photodetectors corresponding to each signal component, being then acquired by a real-time sampling scope and offline processed by each digital signal processing (DSP) stack described in Fig. 2.

As previously discussed, the DSP nonlinear compensation comparison encompass four different approaches, each of them represented by the same color on the block diagram in Fig. 2 and on the final results in Fig. 3(b). As a reference, the linear compensation (LC, blue line) only compensates the chromatic dispersion (CDC) after the pre-processing (normalization, DC-level elimination, and resampling) and orthonormalization of the acquired signals. Following, a dynamic equalization is performed by a radius-directed equalizer (RDE) with a constant modulus algorithm (CMA) to ensure its convergence. Finally, carrier recovery (CR) is performed, allowing the estimation of the  $Q^2$  factor, which is the performance metric for the here proposed investigation. The second DSP stack evaluated (MIMO/MLSE, red line) encompass only the

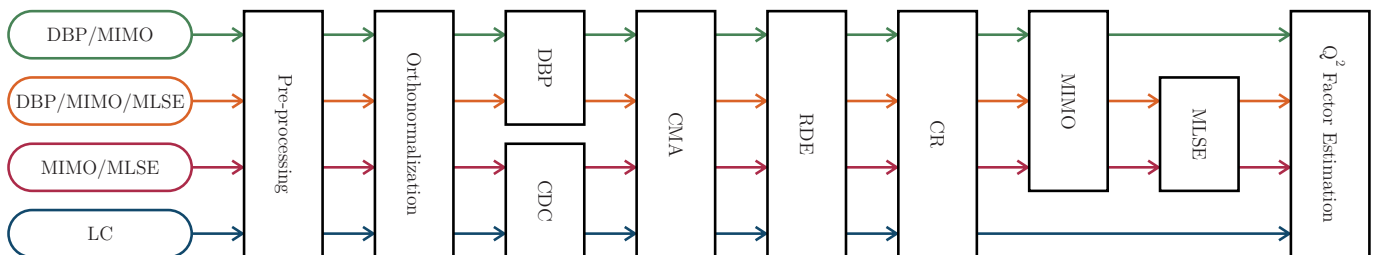
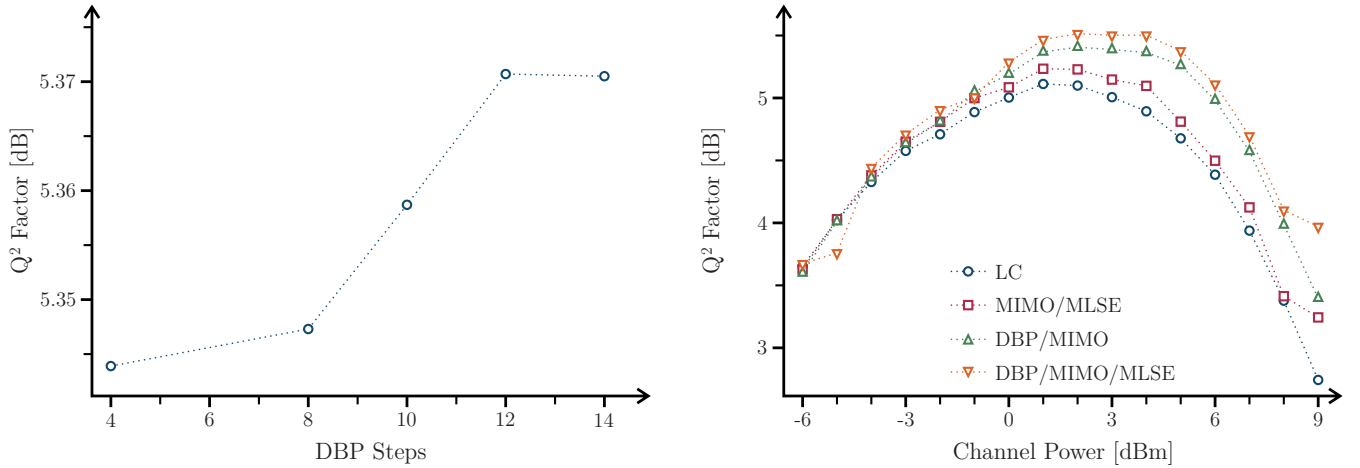


Fig. 2. Digital signal processing (DSP) block diagrams encompassing the different implementations. As a reference, only linear compensation is performed for the LC stack (blue line) with the addition of MIMO and MLSE algorithms (red line). The DBP-based stacks also are performed combined with MIMO equalization, and with (orange line) or without (green line) the MLSE block.



(a) Optimization of the number of steps considered for digital back-propagation algorithm.

(b) Nonlinear compensation performance comparing the four DSP stacks here analyzed.

Fig. 3. Digital back-propagation algorithm optimization and comparative results analyzing the different DSP implementations for nonlinear compensation ranging the launched channel power.

CDC (*i.e.*, without any digital back-propagation algorithm) combined with a  $4 \times 4$  multiple-input multiple-output (MIMO) equalization, followed by a maximum likelihood sequence estimation (MLSE) block, both being executed after carrier recovery. The last two DSP implementations replace the CDC by a digital back-propagation (DBP) algorithm with MIMO equalization, and with MLSE (DBP/MIMO/MLSE, orange line) or without it (DBP/MIMO, green line). For each DSP stack implementation, the system performance is evaluated in terms of  $Q^2$  factor, for channels launch power ranging from  $-6$  dBm up to  $9$  dBm, implying in different levels of nonlinear degradation due to Kerr-related phenomena.

### III. RESULTS

Based on data acquired from the unrepeated transmission employing the experimental setup shown in Fig. 1 and retrieving the transmitted signal through the DSP stacks, depicted in Fig. 2, it is possible to compare the performance of each DSP implementation as presented in Fig. 3. First, in Fig. 3(a), the digital back-propagation algorithm is optimized in terms of number of steps per span, which were uniformly distributed along the first 150 km of the unrepeated link. As the DBP aims to compensate the signal nonlinear degradation, the implementations here employed were applied specifically in the link regions where the transmitted channels attain the highest propagation powers, inducing more severely Kerr-related nonlinear impairments. For the link here analyzed, it occurs close to the transmitter side, specifically in the region where the distributed Raman amplification takes place and right after the remote optically pumped amplifier. In the last 200 km of the unrepeated link, nonlinear impairments are negligible due to the low propagation power of the transmitted channels, sparing nonlinear equalization and requiring only chromatic dispersion compensation. The step size optimization carried out, as the result presented in Fig. 3(a), indicates that the best trade-off between performance and complexity is achieved for 12 steps per fiber span. In a similar way, the

MLSE memory was also previously optimized, being, due to the computational complexity, set to a value of 2.

Finally, employing the DBP and MLSE parameters, properly optimized for each DSP stack, the performance comparison in terms of  $Q^2$  factor is presented in Fig. 3(b), for channel launch powers ranging from  $-6$  dBm up to  $9$  dBm. As it is possible to notice, for launch power below  $-3$  dBm per channel, the nonlinear impairments are negligible and the four DSP stacks attain similar performance. Nonetheless, in this condition, the signals are severely degraded in terms of optical signal-to-noise ratio (OSNR) by the amplified spontaneous emission (ASE) of each amplification stage, resulting in low  $Q^2$  factor. As the launch power increases, the received OSNR and, in consequence, the  $Q^2$  factor improves, indicating a better systemic performance. However, the Kerr-related nonlinear impairments start to significantly impact the transmitted channels, resulting in significant  $Q^2$  gains for the more complex DSP stacks here analyzed, specially the ones based on DBP algorithms. Compared to the reference employing only linear CD compensation (blue line), the inclusion of MLSE equalization (red line) resulted in improvements of 0.1 dB and 1 dB in terms of  $Q^2$  factor and optimum launch power, respectively. Evidently, the application of a DBP algorithm resulted in even higher gains due to its capacity to effectively compensate the channels SPM degradation, resulting in 0.3 dB and 1 dB in terms of  $Q^2$  factor and optimum launch power for the case without MLSE equalization (green line) and 0.4 dB and 2 dB for the case combining DBP, MIMO, and MLSE (orange line). For launch powers above 4 dBm, the transmitted channels  $Q^2$  factor significantly decreases due to the severe degradation from XPM effects, which are not compensated by any of the DSP stacks analyzed in this work. The employment of coupled-equations DBP (CE-DBP) [10] or the ones based on optical phase conjugation (OPC) [11] can attain higher gains at the cost of higher complexity in the DSP and/or in the experimental setup.

## IV. CONCLUSIONS

We experimentally investigated the performance of four DSP stacks combining DBP, MLSE, and MIMO algorithms for nonlinear compensation in unrepeated optical links. The experimental setup encompasses the unrepeated wavelength-multiplexed transmission of  $17 \times 200$ -Gb/s channels (32 GBd DP-16QAM) over 350 km of a heterogeneous link composed of large-effective area and low-loss single-mode fibers with hybrid optical amplification combining conventional EDFAs, DRAs, and ROPAs. The results indicated improvements in  $Q^2$  factor and optimum channel launch power of up to 0.4 dB and 2 dB, compared to the linear CD compensation only, using the combination of DBP, MIMO, and MLSE.

## REFERENCES

- [1] T. Sutili, P. F. Pinto Neto, F. D. Simões, G. J. Suzigan, and R. C. Figueiredo, "Cost-effective solution for high-capacity unrepeated transmission," in *2020 Optical Fiber Communications Conference and Exhibition (OFC)*, March 2020, pp. 1–3, [doi:10.1364/OFC.2020.T4I.4].
- [2] J. C. S. S. Januário, A. Chiuchiarelli, S. M. Rossi, J. H. Cruz Júnior, J. D. Reis, C. Mornatta, A. Festa, and A. C. Bordonalli, "System design for high-capacity unrepeated optical transmission," *Journal of Lightwave Technology*, vol. 37, no. 4, pp. 1246–1253, Feb 2019, [doi:10.1109/JLT.2019.2891078].
- [3] J. H. Cruz Júnior, F. Della Lucia, T. Sutili, D. A. A. Mello, and R. C. Figueiredo, "Gradient-based optimization for unrepeated optical systems," in *2019 SBMO/IEEE MTT-S International Microwave and Optoelectronics Conference (IMOC'2019)*, Aveiro, Portugal, Nov. 2019.
- [4] F. Della Lucia, J. H. da Cruz Júnior, T. Sutili, and R. C. Figueiredo, "Natural computing algorithms for optimization of high-order distributed Raman amplifiers," in *2019 SBMO/IEEE MTT-S International Microwave and Optoelectronics Conference (IMOC'2019)*, Aveiro, Portugal, Nov. 2019.
- [5] J. H. Cruz Júnior, T. Sutili, S. M. Rossi, R. C. Figueiredo, and D. A. de Arruda Mello, "Fast adaptive digital back-propagation algorithm for unrepeated optical systems," in *2020 Optical Fiber Communications Conference and Exhibition (OFC)*, March 2020, pp. 1–3, [doi:10.1364/OFC.2020.T4I.2].
- [6] E. Ip and J. M. Kahn, "Compensation of dispersion and nonlinear impairments using digital backpropagation," *Journal of Lightwave Technology*, vol. 26, no. 20, pp. 3416–3425, 2008, [doi:10.1109/JLT.2008.927791].
- [7] D. Marsella, M. Secondini, and E. Forestieri, "Maximum likelihood sequence detection for mitigating nonlinear effects," *Journal of Lightwave Technology*, vol. 32, no. 5, pp. 908–916, 2014, [doi:10.1109/JLT.2013.2294457].
- [8] F. P. Guimar, L. Bertignono, A. Nespola, P. Poggiolini, F. Forghieri, and A. Carena, "Combining probabilistic shaping and nonlinear mitigation: Potential gains and challenges," in *Optical Fiber Communications Conference and Exposition (OFC)*, 2018, [doi:10.1364/OFC.2018.M3C.3].
- [9] E. P. da Silva, K. J. Larsen, and D. Zibar, "Impairment mitigation in superchannels with digital backpropagation and MLSD," *Optics Express*, vol. 23, no. 23, pp. 29 493–29 501, 2015, [doi:10.1364/OE.23.029493].
- [10] E. Mateo, L. Zhu, and G. Li, "Impact of XPM and FWM on the digital implementation of impairment compensation for WDM transmission using backward propagation," *Optics Express*, vol. 16, no. 20, pp. 16 124–16 137, 2008, [doi:10.1364/OE.16.016124].
- [11] F. Da Ros, M. P. Yankov, E. P. da Silva, M. Lillieholm, P. M. Kaminski, P. Guan, H. Hu, A. T. Clausen, M. Galili, and L. K. Oxenløwe, "Nonlinearity compensation through optical phase conjugation for improved transmission reach/rate," in *2018 20th International Conference on Transparent Optical Networks (ICTON)*, 2018, pp. 1–2, [doi:10.1109/ICTON.2018.8473621].